Countercurrent chromatographic isolation of 11´-γ-tocomonoenol from and detection of novel minor tocochromanols in pumpkin seed oil

Alexander Kröpfl[1] and Walter Vetter[1]

[1]University of Hohenheim

March 4, 2021

Abstract

A non-refined, organic pumpkin seed oil (PSO) was chosen for the isolation and structure verification of the rare vitamin E compound γ-tocomonoenol (γ-T1). Initial measurements indicated the presence of ˜0.4 mg γ-T1 per 100 g pumpkin seed oil. Saponification of ˜2 L pumpkin seed oil, followed by repeated countercurrent chromatography (CCC) with the solvent system *n*-hexane/benzotrifluoride/acetonitrile (10:3.5:6.5, *v*/*v*/*v*) and silica gel column chromatography enabled the isolation of 6.8 mg γ-T1 with a purity of 96.0%. Structural analysis by ^{1}H NMR spectroscopy and gas chromatography with mass spectrometry (GC/MS) of the γ-T1 isolate confirmed the presence of a double bond in C-11´-position (11´-γ-tocomonoenol). Next to γ-T1, CCC fractionation enabled the detection of 18 different tocochromanols, many of which were reported for the first time in pumpkin seed oil. This unmatched variety covered among others α-/γ-tocopherol, α-/γ-tocomonoenol, two α- and two γ-tocodienol isomers, α-/γ-tocotrienol as well as the rare 11´-β-tocomonoenol (β-T1) and δ-T1. Three uncommon tocochromanols were also detected whose origins and structure remained unclear.

1. Introduction

Vitamin E is a collective term for a group of naturally occurring lipophilic antioxidants (Kamal-Eldin et al., 1996). In addition, a variety of beneficial effects on human health have been attributed to this substance class, e.g. prevention of arteriosclerosis (Saremi and Arora, 2010), reduction of blood cholesterol levels (Prasad, 2011), and inhibition of tumour promotion (Goh et al., 1994). Likewise, anti-inflammatory and anti-angiogenetic effects were referred to vitamin E (Birringer et al., 2018; Miyazawa et al., 2004). The common structural feature of vitamin E compounds is a 6-chromanol backbone, and hence individual variants (vitamers) are commonly termed tocochromanols (**Fig. 1**) (Kamal-Eldin et al., 1996). One or two methyl groups in addition to the compulsory one on C-8 of the aromatic ring of the 6-chromanol backbone lead to a theoretical variety of four homologue groups, i.e. α-tocochromanols (5,7,8-trimethyl substituted), β-tocochromanols (5,8-dimethyl substituted), γ-tocochromanols (7,8-dimethyl substituted) and δ-tocochromanols (8-methyl substituted) (Kamal-Eldin et al., 1996; Sen and Khanna, 2006; IUPAC-IUB, 1982). Both a methyl and a branched alkyl substituent (side chain) are attached at $2S$ - and $2R$ -position, respectively, to the heterocyclic ring moiety. The four tocopherols (α-T, β-T, γ-T and δ-T) contain no double bond (db) in the side chain (**Fig. 1a**), whereas the four tocotrienols (α-T3, β-T3, γ-T3 and δ-T3) contain three db (**Fig. 1b**) [1,7,8]. The resulting four tocopherols and four tocotrienols are regarded as the eight original vitamin E forms (Kamal-Eldin et al., 1996). The recommended adequate daily intake was suggested to be ˜8 mg α-T or higher amounts of other tocochromanols which are ˜2-4 times less bioactive (Deutsche Gesellschaft für Ernährung (DGE), 2018).

Recently, tocomonoenols (one db in the side chain, T1, **Fig. 1c**) and tocodienols (two db in the side chain, T2) have been discovered in selected plants. The most prominent representative of these rare tocochromanols

is 11´-α-T1 which was detected especially in palm oil (Matsumoto et al., 1995; Ng et al, 2004) and at traces in sunflower oil (Hammann et al., 2015). Yamamoto et al. (1999) discovered 12´-α-T1 in eggs of the pacific salmon *Oncorhynchus keta* being named marine-derived tocopher. A recent study enabled the differentiation of both isomers, i.e. 11´-α-T1 and 12´-α-T1, by gas chromatography (GC) with mass spectrometry (MS) and nuclear magnetic resonance spectroscopy (NMR) (Müller et al, 2018). Moreover, two α-T2 isomers (i.e. 3´,11´-α-T2 and 7´,11´-α-T2) were successively detected in palm oil (Gee et al., 2016; Müller et al., 2020).

Next to one report on traces of δ-T1 in kiwi fruits (Fiorentino et al, 2009), γ-T1 was found at trace levels in sesame and corn oil (Mariani and Bellan, 1996), green leaves of alligator plant (*Kalanchoe daigremontiana*) (Kruk et al., 2011), as well as with most relevant shares in pumpkin seed oil (PSO) (Butinar et al., 2011). Specifically, Butinar et al. (2011) detected γ-T1 with a content of ˜120 µg/g in roasted seeds of the Slovenian pumpkin variety *Slovenska golica* . The position of the db was provisionally allocated to C-11´-position based on data collected for α-T1 (Ng et al, 2004; Puah et al., 2007) and the diagnostic allylic ion at m/z 69 (Müller et al., 2020; Fiorentino et al, 2009). Moreover, they also tentatively indicated the presence of a γ-T2 isomer in the same samples (Butinar et al., 2011). However, none of the minor γ-tocochromanols were isolated and available in milligram-amounts, which would be important in order to study the bioactivity relative to α-T.

The goal of this study was the isolation as well as the structural characterisation and verification of γ-T1 in high purity from PSO. Given previous experience with the isolation of tocochromanols (Müller et al, 2018; Müller et al., 2020; Vetter et al., (2019), countercurrent chromatography (CCC) appeared to be well-suited for this purpose. Furthermore, CCC fractionation followed by gas chromatography with mass spectrometry (GC/MS) analysis of the individual fractions enabled the detection of more minor lipid components than without this step (Schröder and Vetter, 2012). Hence, this CCC fractionation and GC/MS screening strategy was adopted in order to describe additional minor tocochromanols in PSO including the verification of γ-T2.

2. Materials and methods

2.1 Sample, Chemicals and reagents

Non-refined, organic PSO from pumpkin seeds roasted at ˜110 °C (Bio-Zentrale Naturprodukte, Ulbering, Germany) was purchased in a local supermarket in Stuttgart (Germany). Potassium hydroxide, toluene (99.9%) and hydrochloric acid (concentrated, 32%) were bought from Carl Roth (Karlsruhe, Germany). Methanol (> 99.8%) and n -hexane (> 95%) were ordered from VWR Chemicals (Darmstadt, Germany). Pyridine, ethyl acetate (both distilled before use), trifluorotoluene (benzotrifluoride, BTF, > 99%) and silica gel 60 were from Sigma-Aldrich (Steinheim, Germany). Acetonitrile (99.9%) was bought from Th. Geyer (Renningen, Germany). The trimethylsilylation reagent (99% N,O-bis(trimethylsilyl) trifluoroacetamide and 1% trimethylchlorosilane) was purchased from Supelco (Bellefonte, PA, USA). The internal standard for GC/MS measurements, 5α-cholestane (> 98%), was from Acros Organics (Geel, Belgium). Deuterated chloroform ($CDCl_3$, 99.8%) was ordered from Deutero (Kastellaun, Germany).

2.3 Saponification of the pumpkin seed oil

Forty-four batches (˜40 g each) of PSO, 170 mL 10% potassium hydroxide in ethanol (w/v) and 25 mL 1% pyrogallol in ethanol (w/v) were placed in a three-necked flask equipped with a reflux condenser, a stopper and a glass gas inlet tube. The end of the tube dipped into the solution in order to purge the mixture with nitrogen to avoid oxidative tocochromanol degradation. The solution was heated and saponified for 4 h under reflux. After cooling the reaction flask on crushed ice, the complete solution was transferred into a separatory funnel and the flask was flushed twice with 10 mL water each. Then, 150 mL dest. water, 4 mL concentrated hydrochloric acid and 100 mLn -hexane were added to the separatory funnel and the solution was shaken vigorously for at least 1 min. The upper organic phase was separated and the lower polar phase was extracted three more times with another 100 mL n -hexane, respectively. The combined$n$ -hexane extracts were washed three times with 2% potassium hydroxide in water (w/v), dried with sodium sulfate and filtrated through a folded filter. The solvent was removed by means of a rotary evaporator (40 °C, 200 mbar). The residue was transferred into a 10 mL brown glass vial by means of a Pasteur pipette. For this purpose, two fully drawn pipettes of n -hexane were added in the flask, the flask was closed with a

stopper and vigorously shaken. After this, the entire solution was transferred with another Pasteur pipette into a 10 mL brown glass vial. This procedure was repeated five times and the residue was stored in the refrigerator at 4 °C until further use. Of the 44 repetitions, four batches (total initial amount ˜160 g PSO), respectively, were combined to give between 0.8 and 1 g saponified PSO extract. These eleven samples of PSO extracts of 0.8-1.0 g sample weight were subsequently separated by CCC.

2.4 Countercurrent chromatographic (CCC) separation

CCC separations were performed with a Quickprep MK8 system (AECS, Downend, UK) using the periphery described in details (Englert et al., 2015). Separations were performed using coil 2 in bobbin 1 and coil 3 in bobbin 2 of the CCC system (total volume 236 mL) (Müller et al, 2018). The solvent system *n* -hexane/ACN/BTF (10:6,5:3,5, *v/v/v*) (Müller et al, 2018) was prepared in a 2 L separatory funnel. After equilibration for about 1 h, the lower phase (LP) and the upper phase (UP) were separated and individually degassed in an ultrasonic bath. CCC separation was performed in head-to-tail mode (LP used as mobile phase) which elutes compounds with decreasing polarity (non-polar compounds eluting last). Accordingly, the two coils were entirely filled with the (upper) stationary phase, and rotation was started (870 rpm, maximum speed). External cooling was used to maintain the temperature of the CCC centrifuge at 17 °C. Then, (lower) mobile phase was pumped through the system at 4 mL/min and the effluent was collected in a measuring cylinder until its breakthrough. The volume was noted, and retention of stationary phase S_f was calculated to be 67-72%, respectively. Afterwards, between 0.8 and 1.0 g of saponified PSO extract (section 2.3) was taken up in a mixture of 4.5 mL of both LP and UP and the whole sample was injected via a 10 mL sample loop into the CCC system. After a delay of 50 min, 55 4 mL-fractions were collected in the fraction collector (total run time 105 min). CCC/UV chromatograms were monitored at 290 nm. Collected fractions were carefully evaporated to dryness (evaporator, gentle stream of nitrogen), transferred into 2 mL brown glass GC vials (three times flushed with 0.5 mL*n* -hexane), evaporated again to dryness and weighed. The residue was taken up in 1 mL *n* -hexane. Aliquots of each CCC fraction (equating a final concentration in the measuring solution of ˜100 µg/mL) were trimethylsilylated according to Müller et al. (2014) and analyzed by GC/MS (section 2.5). In total, 11 CCC runs were performed to yield the final amount of 6.8 mg γ-T1.

2.5 *GC/MS analysis of silylated samples*

Tocochromanols and interfering compounds in sample solutions and CCC fractions were analyzed with a 6890/5973N GC/MS system (Agilent Technologies, Santa Clara, CA, USA), equipped with a 30 m x 0.25 mm internal diameter capillary column coated with 0.25 µm 5% diphenyl, 95% dimethyl polysiloxane (Optima 5 HT, Macherey-Nagel, Düren, Germany). The oven program started for 1 min at 55 °C. Then, the temperature was ramped at 20 °C/min to 255 °C, directly at 1.5 °C/min to 283 °C and finally at 15 °C/min to 300 °C which was held for 9 min (total run time 39.8 min). An MPS 2 autosampler (Gerstel, Mulheim, Germany) was used for sample injection (1 µL) in splitless mode. Injector temperature was set to 250 °C. The carrier gas helium (5.0 quality, Westfalen company, Münster, Germany) was transported with a constant flow of 1 mL/min. MS data was collected in full scan mode (m/z 50 to 650) after a solvent delay of either 7.0 min (method A) or 15.0 min (method B). Transfer line, ion source, and quadrupole operated at 280 °C, 230 °C and 150 °C, respectively.

2.6 Column chromatography

CCC fractions with highest purities of γ-T1 according to GC/MS analysis (generally CCC fractions 16-19, partly also CCC fractions 15 and 20 and scarcely CCC fractions 14 and 21) were further purified by column chromatography (1 cm inner diameter glass column filled with 5 g silica gel 60, deactivated with 20% water) according to Hammann et al. (2015). The selection criterion was a maximum of 5% interfering β-/γ-tocochromanols in relation to γ-T1 in the fraction. Selected CCC fractions were transferred to the column using a Pasteur pipette. For this purpose, the complete solution from the 2 mL brown glass GC vial (section 2.4) was individually placed onto the column and the vial was rinsed three more times with 0.5 mL of *n* -hexane. Silica fraction 1 (30 mL *n* -hexane) and silica fraction 2 (40 mL*n* -hexane/ethyl acetate, 99:1, *v/v*) were collected in 100 mL pear shaped flasks. Based on initial trials, the subsequent silica fraction 3 (*n*

-hexane/ethyl acetate, 95:5, *v/v*) was subdivided into six aliquots of different volume, namely fraction 3.1 (0-15 mL), fraction 3.2 (15-17 mL), fraction 3.3 (17-20 mL), fraction 3.4 (20-22 mL), fraction 3.5 (22-25 mL) and fraction 3.6 (25-50 mL). Fractions 3.1 to 3.5 were collected in 20 mL brown glass derivatisation tubes and fraction 3.6 in a 100 mL brown glass pear shaped flask. Finally, more polar compounds were eluted with 40 mL ethyl acetate (silica fraction 4) into a 100 mL pear shaped flask. Fractions 1, 2 and 4 were evaporated to dryness in a rotary evaporator and fractions 3.1-3.6 by means of a gentle stream of nitrogen. Residues of all fractions were taken up with *n* -hexane and transferred into 2 mL brown glass GC vials, respectively. Aliquots were trimethylsilylated and measured by GC/MS (section 2.5).

2.7 ^{1}H NMR spectroscopy

Combined isolates of γ-T1 (obtained after CCC and column chromatography) were evaporated to dryness and the residue (˜5.4 mg) was taken up with $CDCl_3$. ^{1}H NMR measurements (500 MHz) were performed on a Bruker Avance III 500 MHz spectrometer (Rheinstetten, Germany). The ^{1}H NMR spectrum (1024 scans) was evaluated using the Spinworks software (4.0.5, K. Marat, University of Manitoba, Winnipeg/Canada, 2014).

3. Results and discussions

3.1 Initial GC/MS measurements and study design

GC/MS analysis of silylated aliquots of the saponified PSO batches (section 2.3) indicated that tocochromanols contributed with ˜3% to the total peak area (**Fig. 2** , range c). GC/MS chromatograms of the saponified batches did not differ from analytically saponified PSO (data not shown). The most abundant peaks (GC elution range 19-20 min, **Fig. 2** , range b) showed GC/MS spectra similar to squalene (five poorly separated terpenoid peaks with*m/z* 69 as the base peak, followed by *m/z* 81, *m/z* 95 as well as *m/z* 121 and *m/z* 137 at about the same intensity (Hammann et al., 2019)). The shorter retention time range of 10-14 min (**Fig. 2** , range a) featured less prominent isoprenoid compounds with GC/MS spectra similar to phytol (base peak at *m/z* 143 (Vetter et al., 2012)) or farnesol (base peak *m/z* 69, and*m/z* 81, *m/z* 93 and *m/z* 135 (Lee et al., 2007)). Phytol and the other isoprenoids most likely originated from saponified chromophores like protochlorophyll and protopheophytin (Fruhwirth and Hermetter, 2008). In agreement with literature reports (Fruhwirth and Hermetter, 2008), PSO mainly featured Δ7-sterols (**Fig. 2** , range d) and the pattern was dominated by α-spinasterol ([?]7,22-stigmastadienol, **Fig. 2**) which was confirmed by M^+ at *m/z* 484 (two db) and the lack of*m/z* 129 (which indicates absence of a db on C-5 (Goad and Akihisa, 1997)), and presence of *m/z* 213 and *m/z* 255 (characteristic for one db in the B-ring, most likely on C-7) and*m/z* 229 (db on C-25 of the side chain).

The tocochromanol pattern, i.e. γ-T (89.3% of total tocochromanol area) followed by 7.3% α-T, 2.5% γ-T1 and 0.9% α-T1 (**Fig. 2** , range c), agreed well with the one reported by Butinar et al. (2011). The high abundance of squalene and other compounds hindered the detection of further, less abundant tocochromanols in the PSO extract. Compared to that, Butinar et al. also detected low amounts of β-T, δ-T and γ-T3 in PSO (Butinar et al., 2011). The GC/MS spectrum of silylated γ-T1 was similar to the one of silylated γ-T except for the shift of the silylated M^+ to *m/z* 486 (γ-T1) instead of*m/z* 488 (γ-T). Additionally, the allylic ion at *m/z* 69 was visible and produced evidence that the db in the side chain was located at C-11´ (Müller et al., 2020; Fiorentino et al, 2009).

On average, each 40 g batch of PSO (section 2.3) provided ˜0.22 g unsaponifiable extract (˜0.55% yield). Accordingly, four batches of ˜40 g PSO were combined in order to reach the maximum sample load of the CCC system (0.8-1.0 g sample). Based on an estimated tocochromanol contribution of ˜3% to the total peak area in saponified and silylated PSO, ˜30 mg tocochromanols were expected in 1 g saponified PSO. Assuming a contribution of 2.5% to the tocochromanols (see above), the amount of γ-T1 was estimated at ˜0.75 mg in 1 g saponified PSO extract. Hence, eleven CCC runs were carried out in order to obtain amounts of >5 mg γ-T1.

3.2 Detailed analysis of CCC fractions in the elution range of tocochromanols.

Displacement of the stationary phase (on average 72 mL) was in the typical range of the BTF system (Müller et al., 2018). S_f values in all 11 CCC runs ranged from 67% to 72%, thus being sufficiently reproducible (see Electronic Supporting Material (ESM) Fig. S1). However, slight variations in run time and thus slight shifts in the collected fractions from run to run prompted us to normalize data of the individual CCC runs. This was carried out by subtracting the volume of displaced stationary phase ($V_{d,}$ here: 72 mL, as an example) from the total volume of mobile phase (LP) that passed the CCC system at the end of the fraction (V_m). Division of this corrected volume by the total coil volume (V_t, here: 236 mL, section 2.4) resulted in the corrected elution volume (CEV) which is independent of individual run-to-run variations (Eq. 1).

$$\text{CEV} = \frac{V_m - V_d}{V_t} \; x \; 100\% = \frac{V_m - 72\ mL}{236\ mL} \; x \; 100\% \quad (1)$$

with CEV - corrected elution volume in percent; V_m – volume of mobile phase; V_d – volume of displaced stationary phase; V_t: total coil volume

This normalization procedure of Hammann et al. (2013) allowed us to discuss data of all eleven CCC runs universally by means of CEV.

In head-to-tail mode (lower phase mobile), tocochromanol families were found to elute in the order T3 < T2 < T1 < T [14]. In addition, according to the recently presented equivalent chain length (ECL) rule of tocochromanols, the effect of one db in the side chain corresponded with one methyl group in the 6-chromanol moiety (Vetter et al., 2019). Hence, γ-T1 was expected to co-elute with δ-T and α-T2 (i.e. between α-T3 and α-T1; CEV: ˜80%,**Fig. 3**). In order to elute all relevant tocochromanols, CCC fractions were collected between 50-105 min (57-150% CEV). As a benefit, the most prominent squalene-like compounds eluted into the post run fraction and thus could be removed.

Early tocochromanol-containing CCC fractions (57-75% CEV) also featured the more abundant isoprenoid compounds. Hence, purity of the first eluting tocochromanol γ-T3 (**1**) (58-74% CEV, **Fig. 3**) whose identity could be verified with a commercial reference standard, was only ˜0.3%, although no other tocochromanols were detected in this CCC elution range. Similarly, the purity of the rare δ-T1 (**2**) (67-97% CEV) was also low but GC/MS analysis of the silylated main fraction (72-74% CEV) allowed its identification via (i) M^+ at *m/z* 472 (base peak, **Fig. 4a**), (ii) the diagnostic tropylium cation at *m/z* 209 and (iii)*m/z* 69, indicating the position of the db at C-11´ (Fiorentino et al, 2009). The elution range of δ-T1 also featured two γ-T2 isomers (γ-T2 isomer 1 (**3**), 67-81% CEV and γ-T2 isomer 2 (**4**), 67-84% CEV, **Fig. 3**) based on *m/z* 484 (M^+, silylated, **Fig. 4,3** ,**4**) and the tropylium cation at *m/z* 223. Both γ-T2 isomers featured the diagnostic allylic ion at *m/z* 69 which indicated that the remote db was located on C-11´ (Müller et al., 2020; Butinar et al., 2011). Also, the difference in GC retention times (Δt_R) of 0.7 min (24.2 min for γ-T2 isomer 1, 24.9 min for γ-T2 isomer 2) was similar to the gap between two α-T2 isomers recently discovered in palm oil, namely 3´,11´-α-T2 and 7´,11´-α-T2 (Müller et al., 2020). This analogy produced evidence that the two γ-T2 isomers in PSO were 3´,11´-γ-T2 (isomer 1) and 7´,11´-γ-T2 (isomer 2), respectively. As described by Müller et al. (2020), isomers with db closer to the 13´-end of the side chain usually elute later from GC columns.

However, the PSO sample featured further uncommon tocochromanols. Compounds **5** (t_R 25.13 min, 70-74% CEV) and**6** (t_R 25.28 min, 72-74% CEV) shared the CCC elution range with the γ-T2 isomers. M^+ at *m/z*486 and the diagnostic (silylated) tropylium cation at *m/z*222/223 indicated the presence of uncommon β- or γ-T1 isomers (β-/γ-$T1_u$). This is remarkable because the classic γ-T1 (**7**) and β-T1 (**9**) isomers were additionally detected in the sample. Compared to them, the uncommon T1 isomers (**5** ,**6**) did not elute according to the ECL rule of tocochromanols (Vetter et al., 2019) and also the GC retention time was higher than expected. Therefore, the substitution pattern in the aromatic ring of the T1 isomers (**5** ,**6**) could not be established this time. Abundant low mass fragment ions at *m/z*69,73, 81 and 143 indicated co-elution with isoprenoid substances.

Next in elution was the target compound γ-T1 (**7**) as well as α-T3 (**8** ; 72-82% CEV) which was verified by means of a reference standard. γ-T1 (t_R: 23.77 min, 72-101% CEV) was identified by means of the silylated M^+ at*m/z* 486 (**Fig. 5** , **7**) which is two atom mass units (2 u) less in comparison with γ-T. Additionally,

presence of*m/z* 69 indicated that the db was located on C-11´. Recently, it was found that the ratio between *m/z* 222 and *m/z* 223 in the GC/MS spectra can be used to distinguish silylated γ- from β-tocopherol (Hammann et al, 2019). Namely, a higher abundance of*m/z* 223 compared to *m/z* 223 was characteristic for silylated γ-T (**Fig. 6d** , **14**) while similarly high abundance of *m/z* 222 and *m/z* 223 was characteristic for silylated β-T (**Fig. 6e** , **15**) (Hammann et al, 2019). Notably, this difference was recently found to be valid for silylated β- and γ-tocochromanols with unsaturated side chain (Müller et al., 2020), and it was also verified in all GC/MS spectra of silylated β-T, γ-T, and other β- and γ-tocochromanols detected in this study. Accordingly, the higher abundance of *m/z* 223 compared to *m/z 2* 22 in the GC/MS spectrum of silylated **7** and the fact that β-tocochromanols elute earlier from the GC column than γ-tocochromanols, further verified that the target compound was rather γ-T1 than β-T1 (11´-β-T1, **9** , t_R 23.44 min, 75-92% CEV) which was also detected in the sample.

Presence of β-T1 (**9**) has been only mentioned twice before in the literature (Müller et al., 2020; Kruk et al., 2011). The slightly earlier GC/MS elution compared to γ-T1, M^+ at*m/z* 486, similar abundance of *m/z* 222 and *m/z* 223, and presence of *m/z* 69 (**Fig. 5** , **9**) produced strong evidence for its presence in the PSO. Likewise, Δt_R between the potential 11´-β-T1 and 11´-γ-T1 was equivalent to Δt_R between β-T and γ-T, providing further evidence for the presence of 11'-β-T1.

In agreement with predictions, the known δ-T (**10**) co-eluted with γ-T1 contributing up to ˜11% to total tocochromanol area in this range. Surprisingly, three more tocochromanols preceded the elution of γ-T (**14**) which was expected to elute next from the CCC system. The first one of these unexpected compounds (**11** , t_R 24.06 min, 77-92% CEV) featured M^+ at *m/z* 488.4 which is isomeric with β- and γ-T, respectively. However, this is curious because only these two T isomers with two methyl groups in the aromatic ring can exist in theory. Nevertheless, compound **11** featured the diagnostic (silylated) tropylium cation at *m/z* 222/223 which supported the presence of a 6-chromanol moiety with two methyl groups in the aromatic part. This uncommon T_u (**11**) showed*m/z* 222 and *m/z* 223 (the higher abundance of *m/z*222 was more similar to β-T than γ-T) and it also featured the weakly prominent *m/z* 263 which is formed by β-/γ-tocochromanols by removal of the entire alkyl chain (**Fig. 6a**). Accordingly, the GC/MS spectrum of silylated T_u (**11**) was similar to silylated β-T (**15** , t_R 22.53 min) and γ-T (**14** , t_R 22.79 min), but T_u(**11**) eluted much later t_R (and even after γ-T1 ((7), t_R: 23.77) (**Fig. 5**). Notably, the shift toward longer t_R of T_u in GC/MS (1.53 min and 1.27 min relative to β-/γ-T) was similar to Δt_Rbetween the uncommon T1 isomers **5** and **6** and β-/γ-T1. T_u (**11**) also eluted earlier from the CCC system than anticipated, namely together with δ-T (**10**) and β-T1 (**9**) (**Fig. 3**), which was also observed for the T1 isomers **5** and **6** . This pointed towards a structural relationship of compounds T_u (**11**), **5**and **6** , which was, however, different to classic tocochromanols. One structural option might be formylated tocochromanols, which were isolated by Merza et al. from the stem bark of mangosteen tree*Garcinia virgata* (Merza et al., 2004) but another option will be discussed below.

In addition, compounds **12** and **13** could be verified to be 3´,11´-α-T2 (**12** , t_R: 27.73 min, 81-92% CEV) and 7´,11´-α-T2 (**13** , t_R 28.50 min, 84-92% CEV) due to identical features as described by Müller et al. who characterized these two 11´-α-T2 isomers in palm oil (Müller et al., 2020). Accordingly, the occurrence of two T2 isomers – if T2 is present – seems to be rather usual.

Presence of γ-T (**14** , 86-150% CEV), β-T (**15** , 89-114% CEV) and the common 11´-α-T1 (**16** , 89-116% CEV) could be identified by means of authentic reference standards (Müller et al., 2018; Vetter et al., 2019). Similarly to observations of Müller et al. (2018) in palm oil, 11´-α-T1 was accompanied by much lower amounts of 12´-α-T1 (**17** , t_R 26.83 min, 99-101% CEV, M^+ *m/z* 500, no *m/z* 69). Compared to the α-T1 isomers (small difference in t_R), the two β-/γ-T1 isomers **3** and **4** discussed before showed a much higher Δt_R which produced strong evidence that both were more different in structure. Finally, α-T (**18** , 109-150% CEV) was the last tocochromanol detected in the sample whose late elution is in agreement with the maximum number of methyl groups in the aromatic part and the lack of double bonds in the side chain (**Fig. 1a**). Accordingly, all naturally occurring families of α-tocochromanols and γ-tocochromanols (T, T1, T2, T3) were present in PSO. Up to now, this variety, including several new detected tocochromanols is unique

for plant oils.

Notably, PSO used for this study was a cold pressed oil from roasted pumpkin seeds. During roasting, pumpkin seed kernels are exposed to temperatures >100 °C and typically at 110 °C under mild conditions (Fruhwirth and Hermetter, 2008). This temperature was confirmed in correspondence with the manufacturer of the used PSO. In view of this thermal treatment, it cannot be excluded that the three uncommon compounds T_u (**11**), **5** and**6** , were formed as artefacts during the roasting of the oil. Presence of a much higher number of tocochromanol isomers in dietary supplement capsules from rice bran oil had already indicated the lability of vitamin E compounds during the refining process (Hammann et al., 2016). However, it must be noted that conditions during refining are significantly harsher than the roasting conditions of the PSO used in this study (Van Hoed et al., 2006). Irrespective of the unsolved origins of compounds T_u (**11**), **5** and**6** , 15 tocochromanols were found to be native constituents of PSO, and many of them were detected for the first time (**Tab. 1**).

3.3 Πυριφιςατιον οφ γ-τοςομονοενολ βψ ςολυμν ςηροματογραπηψ

Depending on CCC fraction and CCC run, the purity of γ-T1 (**7**) ranged only between 3.3% and 17.8% after CCC separation. This was mostly due to the low share of γ-T1 in the sample. More abundant compounds result in broader peaks which are overlapping with minor compounds such as γ-T1 in the present case (Müller et al., 2019).

Specifically, the presence of high amounts of phytol-like compounds in some CCC fractions reduced the purity of γ-T1. With regard to tocochromanols, γ-T1 was usually predominant (maximum share 93.5%), followed by δ-T and β-T1. Yet, these two tocochromanols show the same ECL as γ-T1 which makes it difficult to separate them by CCC (Vetter et al., 2019). Hence, highly pure γ-T1 could not be obtained by CCC alone but required rather a complementary method with orthogonal separation characteristics. Recently, Müller et al. showed that column chromatography eluted tocochromanols predominantly according to the methylation pattern on the 6-chromanol ring, specifically in the order α- < β- and γ- < δ-tocochromanols (Müller et al., 2020). Our initial tests confirmed this because - contrary to CCC - γ-T (**14**), γ-T1 (**7**) and γ-T3 (**1**) could not be separated by column chromatography. Especially, presence of γ-T (**7**) which showed a very broad elution range in CCC due to its high concentration was a problem in late CCC fractions (**Fig. 3**). Likewise, presence of β-T1 (**9**) was unfavourable, because it could not be separated from γ-T1 by column chromatography. Therefore, only CCC fractions comparably rich in γ-T1 (**7**) but with negligible amounts of β-T1 (**9**) and γ-T (**14**) were considered for the isolation. This prerequisite was fulfilled with CCC fractions with 82-89% CEV in order to reach a purity of >95% γ-T1 (**Fig. 3** , dotted lines). Though, this constraint implied that a large share of γ-T1 could not be pooled.

For the majority of CCC runs, CEV range 81-91% was also suitable and in some runs the range 79-92%, additionally. Due to the presence of more abundant phytol- and farnesol-related compounds (section 3.2), the amount of γ-T1 (**7**) was only 0.01-0.51 mg. However, these major compounds still had a strong impact because the capacity of the column was only ˜2 mg. Therefore, suitable CCC fractions could not be pooled but had to be chromatographed individually. While hydrocarbons like squalene (elution into fraction 1) (Hammann et al., 2015) could be separated, phytol-like substances and shares of the farnesol-like compounds (parts eluting into silica fraction 4) were also detected into the tocochromanol fraction 3. Therefore, silica fraction 3 was subdivided into six sub-fractions according to Müller et al. (Müller et al., 2018) (section 2.6) with slight modifications. Subsequent GC/MS analysis of the silylated silica fractions showed that γ-T1 (**7**) eluted mainly into silica fraction 3.6 which also contained the majority of impurities (**Fig. 7**). Hence, purity of γ-T1 in fraction 3.6 only was between ˜1% (**Fig. 7a**) and ˜25% (**Fig. 7b**). Despite some variations from run to run (**Fig. 7**), the purity of fractions 3.3, 3.4 and 3.5 was usually >95% (**Fig. 7**). Accordingly, this fractionation scheme was applied to all suitable CCC fractions from different CCC runs, and fractions 3.3, 3.4, and 3.5 were measured by GC/MS and pooled if pure enough, while silica fractions 3.2 and 3.6 were combined and chromatographed again. Altogether, ˜45 separations on the silica column were carried out, each of which allowed to collect between 0.06 mg to 0.18 mg of highly pure γ-T1 (**7**). Finally, CCC and column chromatography provided 6.8 mg γ-T1 (**7**) with a purity of 96.0%. Minor impurities originated

from traces of β-T1, γ-T (**Fig. 8**) and two phytol-like compounds. Hence, the expenditure in the lab was very high (saponification of ˜2 L PSO, eleven CCC runs, 45 silica columns, >250 GC/MS runs). However, the goal could be reached and the isolate of γ-T1 (**7**) could be subjected to NMR analysis.

3.4 Στρυστυρε δετερμινατιον οφ γ-T1 βψ ^{1}H NMP σπεστροσοπψ ανδ Γ˜/ΜΣ δατα

The bulk of isolated γ-T1 (5.4 mg) was analyzed by ^{1}H NMR analysis (section 2.7). In the downfield range, the singlet at 6.30 ppm confirmed the presence of one proton on C-5 in the aromatic part of the 6-chromanol ring (**Fig. 9a**). This chemical shift was slightly upfield compared to 6.40 ppm in the ^{1}H NMR spectrum of γ-T3 which was measured under the same conditions for comparison. This is in accordance with literature data for a proton on C-5 at 6.38 ppm (γ-T3) (Ohnmacht et al., 2008) and 6.37 ppm (γ-T), respectively (Baker and Myers, 1991). Compared to that, a proton on C-7 (β-T3) was expected more downfield at 6.48 ppm (Ohnmacht et al., 2008) or at 6.46 (β-T), respectively (Baker and Myers, 1991). This confirmed our assignments by GC/MS via (the silylated) M^+ atm/z 486 and m/z 223 > m/z 222 (section 3.2).

Furthermore, only one signal (triplets of triplet, J = 7.13 Hz, 1.25 Hz) was detected in the range of olefinic protons at 5.033 ppm. Accordingly, the second sp^2 hybridized carbon did not carry a proton (which is true when located on a branching point). Also, large coupling indicated a regular ^3J -coupling between C-10´and C-11´ and a long-range coupling between C-9´and C-11´. Such a scenario can only be found when the double bond is located in either C-3´-, C-4´-, C-7´-, C-8´- or C-11´-position, respectively. Assuming a natural substitution pattern, the double bond would be expected in C-11´-position while exclusive presence in C-7´-position was rather unlikely. However, the presence on C-3´-position could not be fully excluded at this point. In the case of α-T2, db positions could be distinguished by means of the signal of C-3 at ˜2.6 ppm for no double bond in C-3´ and ˜2.7 ppm for one db on C-3´ (Müller et al., 2020). Contrary to (expected) triplets as in the case of α-tocochromanols, the multiplet at ˜2.6 ppm looked more like a quartet in γ-tocochromanols, although the integral (I = 2) was the same as expected. The fact that the same multiplet was also observed in the ^{1}H NMR spectrum of γ-T3 (and γ-T) produced evidence that both protons on C-3 of γ-tocochromanols were not isochronous. Non-constant distances between the individual signals confirmed this difference between α- and γ-tocochromanols. Most importantly, however, compared to γ-T3, the mulitplet of γ-T1 was shifted highfield by ˜0.1 ppm (**Fig** . **9c**and **9d**) which verified the absence of a db in C-3´-position (Müller et al., 2020). This was further supported by a singlet at ˜1.62 ppm originating from the methyl group in C-13´ position. For α-tocochromanols, Müller et al. (2020) observed a singlet at ˜1.70 ppm when it is close to a double bond in C-11´-position. In case of γ-T1, this singlet was slightly shifted upfield but the ratio of the integrals of 2:3 compared to the multiplet at 2.70 ppm agreed well with literature data. Therefore, the db was confirmed to be on C-11´-position. This is in agreement with GC/MS data of silylated γ-T1 which featured the diagnostic fragment ion atm/z 69. Hitherto, m/z 69 was detected in all unsaturated tocochromanols detected in plants (tocomonoenols, tocodienols and tocotrienols) but not in tocopherols and marine-derived tocopherols with the db on C-12´. Hence, the terminal double bond seems to be obligate in unsaturated plant tocochromanols.

4. Conclusion

Once again, CCC proved to be a powerful technique for both the enrichment of minor compounds from lipid extracts and discovery of trace components in lipid matrices. With regard to the latter point, 18 tocochromanols were detected in the pumpkin seed oil (PSO). However, for three compounds it remained unclear if these were hitherto unknown naturally occurring tocochromanols or artefacts formed during the roasting process involved in the processing of the oil. Even without these compounds, the number of tocochromanols detected in the sample surpassed results from any previous study on PSO or other natural oils.

While CCC allowed to enrich γ-T1 from the oil, a full isolation of this minor compound in the oil (˜0.4 mg/100 g) in high purity could not be achieved. However, the subsequent column chromatography which was based on a different separation principle allowed to gain 6.8 mg γ-T1 with 96% purity. Admittedly, the expenditure (44 saponifications, 11 CCC runs, ˜45 column chromatographic separations) was high, but the isolation of γ-T1 may also be useful in studies of its biological activity. Recently, α-T1 was found to behave

differently to both α-T and α-T3 (Irías-Mata et al., 2020). For example, it does not seem to entirely depend on α-tocopherol transfer protein (TTP) function for its secretion into the systemic circulation (Irías-Mata et al., 2020). Similar studies with γ-T1 would ultimately support the understanding of minor tocochromanols.

References

1. Baker, J. K., & Myers, C.W. (1991). One-dimensional and two-dimensional ^{1}H- and^{13}C-nuclear magnetic resonance (NMR) analysis of vitamin E raw materials or analytical reference standards.*Pharmaceutical Research* , **8** :763–770. https://doi.org/10.1023/A:1015810303089
2. Birringer, M., Siems, K., Maxones, A., Frank, J., & Lorkowski, S. (2018). Natural 6-hydroxychromanols and -chromenols: structural diversity, biosynthetic pathways and health implications. *RSC Advances* , **8** :4803–4841. https://doi.org/10.1039/C7RA11819H
3. Butinar, B., Bučar-Miklavčič, M., Mariani, C., & Raspor, P. (2011). New vitamin E isomers (gamma-tocomonoenol and alpha-tocomonoenol) in seeds, roasted seeds and roasted seed oil from the Slovenian pumpkin variety '*Slovenska golica* '. *Food Chemistry,***128** :505–512. https://doi.org/10.1016/j.foodchem.2011.03.072
4. Deutsche Gesellschaft für Ernährung (DGE), Österreichische Gesellschaft für Ernährung (ÖGE), Schweizerische Gesellschaft für Ernährung (SGE). (2018). D-A-CH-Referenzwerte für die Nährstoffzufuhr (2nd ed., 4th updated version). Bonn, Germany. Retrieved from https://www.dge.de/wissenschaft/referenzwerte/vitamin-e/?L=0
5. Englert, M., Brown L., & Vetter, W. (2015). Heart-cut two-dimensional countercurrent chromatography with a single instrument.*Analytical Chemistry* , **87** :10172–10177. https://doi.org/10.1021/acs.analchem.5b02859
6. Fiorentino, A., Mastellone, C., D'Abrosca, B., Pacifico, S., Scognamiglio, M., Cefarelli, G., Caputo, R., & Monaco, P. (2009). δ-Tocomonoenol. A new vitamin E from kiwi (*Actinidia chinensis*) fruits. *Food Chemistry* , **115** :187–192. https://doi.org/10.1016/j.foodchem.2008.11.094
7. Fruhwirth, G., & Hermetter, A. (2008). Production technology and characteristics of Styrian pumpkin seed oil. *European Journal of Lipid Science and Technology* , **110** :637–644. https://doi.org/10.1002/ejlt.200700257
8. Gee, P. T., Liew, C. Y., Thong, M. C., & Gay, M. C. L. (2016). Vitamin E analysis by ultra-performance convergence chromatography and structural elucidation of novel α-tocodienol by high-resolution mass spectrometry. *Food Chemistry* , **196** :367–373. https://doi.org/10.1016/j.foodchem.2015.09.073
9. Goad, J. L., & Akihisa, T. (1997). Analysis of sterols (1st ed.). London, UK:Blackie Academic & Professional.
10. Goh, S. H., Hew, N. F., Norhanom, A. W., & Yadav, M. (1994). Inhibition of tumour promotion by various palm-oil tocotrienols.*International Journal of Cancer* , **57** :529–531. https://doi.org/10.1002/ijc.2910570415
11. Hammann, S., Englert, M., Müller, M., & Vetter, W. (2015). Accelerated separation of GC-amenable lipid classes in plant oils by countercurrent chromatography in the co-current mode.*Analytical and Bioanalytical Chemistry* , **407** :9019–9028. https://doi.org/10.1007/s00216-015-9068-5
12. Hammann, S., Korf, A., Bull, I. D., Hayen, H., & Cramp, L. J. E. (2019). Lipid profiling and analytical discrimination of seven cereals using high temperature gas chromatography coupled to high resolution quadrupole time-of-flight mass spectrometry. *Food Chemistry* ,**282** :27–35. https://doi.org/10.1016/j.foodchem.2018.12.109
13. Hammann, S., Kröpfl, A., & Vetter, W. (2016). More than 170 polyunsaturated tocopherol-related compounds in a vitamin E capsule: countercurrent chromatographic enrichment, gas chromatography/mass spectrometry analysis and preliminary identification of the potential artefacts. *Journal of Chromatography A* , **1476** :77–87. https://doi.org/10.1016/j.chroma.2016.11.018
14. Hammann, S., Tillmann, U., Schröder, M., & Vetter, W. (2013). Profiling the fatty acids from a strain of the microalgae*Alexandrium tamarense* by means of high-speed counter-current chromatographyand gas chromatography coupled with mass spectrometry.*Journal of Chromatography A* , **1312** :93-103. https://doi.org/10.1016/j.chroma.2013.08.090

15. Hammann, S., Wendlinger, C., & Vetter, W. (2015). Analysis of intact cholesteryl esters of furan fatty acids in cod liver. *Lipids* ,**50** :611–620. https://doi.org/10.1007/s11745-015-4019-7
16. Irías-Mata, A., Sus, N., Hug, M.-L., Müller, M., Vetter, W., & Frank, J. (2020). α-Tocomonoenol is bioavailable in mice and may partly be regulated by the function of the hepatic α-tocopherol transfer protein. *Molecules* , **25** :4803. https://doi.org/10.3390/molecules25204803
17. IUPAC-IUB Joint Commission on Biochemical Nomenclature. Nomenclature of tocopherols and related compounds. (1982). *Pure and Applied Chemistry* , 54:1507–1510.
18. Kamal-Eldin, A., & Appelqvist, L-Å. (1996). The chemistry and antioxidant properties of tocopherols and tocotrienols. *Lipids* ,**31** :671–701. https://doi.org/10.1007/BF02522884
19. Kruk, J., Pisarski, A., & Szymańska, R. (2011). Novel vitamin E forms in leaves of *Kalanchoe daigremontiana* and *Phaseolus coccineus* . *Journal of Plant Physiology* ,**168** :2021–2027. https://doi.org/10.1016/j.jplph.2011.06.015
20. Lee, H., Finckbeiner, S., Yu, J. S., Wiemer, D. F., Eisner, T., & Attygalle, A. B. (2007). Characterization of (E,E)-farnesol and its fatty acid esters from anal scent glands of nutria (*Myocastor coypus*) by gas chromatography–mass spectrometry and gas chromatography–infrared spectrometry.*Journal of Chromatography A* , **1165** :136–143. https://doi.org/10.1016/j.chroma.2007.06.041
21. Mariani, C., & Bellan, G. (1996). Content of tocopherols, deidrotocopherols, tocodienols, tocotrienols in vegetable oils.*Rivista Italiana delle Sostanze Grasse* , **73** :533–543.
22. Matsumoto, A., Takahashi, S., Nakano, K., & Kijima, S. (1995). Identification of new vitamin E in plant oil. *Journal of Oleo Science* , **44** :593–597.
23. Merza, J., Aumond, M.-C., Rondeau, D., Dumontet, V., Le Ray, A.-M., Se´raphin, D., & Richomme, P. (2004). Prenylated xanthones and tocotrienols from *Garcinia virgata* . *Phytochemistry* ,**65** :2915–2920. https://doi.org/10.1016/j.phytochem.2004.06.037
24. Miyazawa, T., Tszuzuki, T., Nakagawa, K., & Igarashi, M. (2004). Antiangiogenic potency of vitamin E. *Annals of the New York Academy of Sciences,* **1031** : 401–404. https://doi.org/10.1196/annals.1331.057
25. Müller, M., Hammann, S., & Vetter, W. (2018). Countercurrent chromatographic isolation and purification of 11'-α-tocomonoenol from the vitamin E extract of palm oil. *Food Chemistry* ,**256** :327–332. https://doi.org/10.1016/j.foodchem.2018.02.133
26. Müller, M., Kröpfl, A., & Vetter, W. (2020). Identification of two α-tocodienol isomers in palm oil after countercurrent chromatographic enrichment. *Analytical and Bioanalytical Chemist* ,**412** :795–802. https://doi.org/10.1007/s00216-019-02303-1
27. Müller, M., Muric, M., Glanz, L., & Vetter, W. (2019). Improving the resolution of overlapping peaks by heartcut two-dimensional countercurrent chromatography with the same solvent system in both dimensions. *Journal of Chromatography A* ,**1596** :142–151. https://doi.org/10.1016/j.chroma.2019.03.012
28. Ng, M. H., Choo, Y. M., Ma, A. N., Chuah, C. H., & Hashim, M. A. (2004). Separation of vitamin E (tocopherol, tocotrienol, and tocomonoenol) in palm oil. *Lipids* , **39** :1031–1035. https://doi.org/10.1007/s11745-004-1327-y
29. Ohnmacht, S., West, R., Simionescu, R., & Atkinson, J. (2008). Assignment of the ^{1}H and ^{13}C NMR of tocotrienols. *Magnetic Resonance in Chemistry* ,**46** :287–294. https://doi.org/10.1002/mrc.2176
30. Prasad, K. (2011). Tocotrienols and cardiovascular health.*Current Pharmaceutical Design* , **17** :2147–2154. https://doi.org/10.2174/138161211796957418
31. Puah, W. C., Choo, M. Y., Ma, N. A., & Chuah, H. C. (2007). The effect of physical refining on palm vitamin E (tocopherol, tocotrienol and tocomonoenol). *American Journal of Applied Sciences* ,**4** :374-377.
32. Saremi, A., & Arora, R. (2010). Vitamin E and cardiovascular disease.*American Journal of Therapeutics* , **17** :56–65. https://doi.org/10.1097/MJT.0b013e31819cdc9a
33. Schröder, M., & Vetter, W. (2012). Investigation of unsaponifiable matter of plant oils and isolation of eight phytosterols by means of high-speed counter-current chromatography. *Journal of Chromatography A* , **1237** :96-105. https://doi.org/10.1016/j.chroma.2012.03.033
34. Sen, C.K., Khanna, S., & Roy, S. (2006). Tocotrienols: vitamin E beyond tocopherols. *Life Sciences* , **78** :2088–2098. https://doi.org/10.1016/j.lfs.2005.12.001

35. Van Hoed, V., Depaemelaere, D., Ayala, J. V., Santiwattana, P., Verhé, R., & DeGreyt, W. (2006). Influence of chemical refining on the major and minor components of rice brain oil. *Journal of the American Oil Chemists' Society* , **83** :315–321. https://doi.org/10.1007/s11746-006-1206-y
36. Vetter, W., Müller, M., Sommer, K., Schröder, M., & Hammann, S. (2019). Development of equivalent chain length (ECL) rules for lipid compounds. *Journal of Chromatography A* , **1599** :187–95. https://doi.org/10.1016/j.chroma.2019.04.042
37. Vetter, W., Schröder, M., & Lehnert, K. (2012). Differentiation of refined and virgin edible oils by means of the *trans* - and*cis* -phytol isomer distribution. *Journal of Agricultural and Food Chemistry* , 60:6103-6107. https://doi.org/10.1021/jf301373k
38. Yamamoto, Y., Maita, N., Fujisawa, A., Takashima, J., Ishii, Y., & Dunlap, W. C. A. (1999). New vitamin E (α-tocomonoenol) from eggs of the Pacific salmon *Oncorhynchus keta* . *Journal of Natural Products* , **62** :1685–1687. https://doi.org/10.1021/np990230v

Tables

Table 1 List of all tocochromanols detected in the pumpkin seed oil (PSO) used for the fractionation and isolation of γ-T1 with information on previous detection and detectability before/after the CCC fractionation

tocochromanol	first detection in PSO	only visible after CCC separation
α-T		
α-T1		
α-T1 ισομερ	yes	yes
α-T2 ισομερ 1	yes	yes
α-T2 ισομερ 2	yes	yes
α-T3	yes	yes
β-T		yes
T_u[a]	yes	yes
β-T1	yes	yes
β-/γ-$T1_\cup$ 1[α]	yes	yes
β-/γ-$T1_\cup$ 2[α]	yes	yes
γ-T		
γ-T1		
γ-T2 ισομερ 1	yes	yes
γ-T2 ισομερ 2		yes
γ-T3		yes
δ-T		yes
δ-T1	yes	yes

[a] potential artefact from the production (roasting) of the PSO

Captions to Figures

Fig. 1 General structure of (**a**) tocopherols (T), (**b**) tocotrienols (T3) and (**c**) tocomonoenols (T1) (Kamal-Eldin, 1996; Saremi and Arora, 2010)

Fig. 2 GC/MS full scan chromatogram of the pumpkin seed oil (PSO) extract after saponification reaction and trimethylsilylation with: (**a**) isoprenoidic compounds similar phytol and farnesol; (**b**) squalene-like terpenoids and 5α-cholestane as internal standard (ISTD); (**c**) tocochromanols including γ-T, γ-T1, α-T and α-T1; (**d**) sterols

Fig. 3 CCC elution profile of all 18 detected tocochromanols in saponified pumpkin seed oil (PSO) after fractionation in head-to-tail mode using the BTF solvent system. Bubble sizes correlates with corrected

GC/MS peak area of the corresponding CCC fractions. The doted area highlights the optimum range for the isolation of γ-T1

Fig. 4 (**a**) GC/MS full scan chromatogram of the silylated CCC fraction with corrected elution volume (CEV) 72-74% and GC/MS spectra of silylated (**b**) δ-T1 (**2**), (**c**) γ-T2 isomer 1 (3), (**d**) γ-T2 isomer 2 (**4**), (**e**) uncommon T1 isomer 1 (**5**), (**f**) uncommon T1 isomer 2 (**6**)

Fig. 5 GC/MS full scan chromatogram of the silylated CCC fraction of saponified pumpkin seed oil (PSO) extract with corrected elution volume (CEV) 89-91% and GC/MS spectra of silylated (**b**) γ -T1 (**7**), (**c**) 11´-β-T1 (**9**), (**d**) α-T2 isomer 1 (**12**) and (**e**) α-T2 isomer 2 (**13**)

Fig. 6 (**a**) GC/MS fragmentation of silylated tocopherols and (**b**) formation of the diagnostic 3-methylbut-2-en-1-ylium cation along with GC/MS spectra of the silylated CCC fraction with corrected elution volume (CEV) 89-91% of saponified pumpkin seed oil (PSO) extract of (**c**) the uncommon tocopherol T_u, (**d**) γ-tocopherol and (**e**) β-tocopherol

Fig. 7 Representative elution scheme of fractions 3.1, 3.2, 3.3, 3.4, 3.5, 3.6, and 4 collected by column chromatography with silica and elution with *n* -hexane/ethyl acetate (95:5, *v/v*) in case of (**a**) high and (**b**) low shares of interfering substances. I1: impurity 1, I2: impurity 2, γ-T1: γ-tocomonoenol, I3: impurity 3

Fig. 8 GC/MS full scan chromatogram of silylated (**a**) γ-T1 isolate after chromatography on a silica column with (**b**) enlarged central part showing minor impurities in form of silylated γ-T and β-T1 and (**c**) mass spectrum of silylated γ-T1

Fig. 9 Excerpts of ^{1}H NMR spectra (500 MHz, 1024 scans) of 11´-γ-T1 with (**a**) the singlet at ˜6.30 ppm (proton at C-5 of the 6-chromanol ring), (**b**) a triplet at ˜5.03 ppm for the proton on C-11´ of the phytylic side chain, and (**c**) the multiplet at ˜2.60 ppm. (**d**) shows the multiplet at ˜2.70 ppm in the ^{1}H spectrum of γ-T3 measured with the same conditions for comparison

Statement

All relevant data is presented in the manuscript or shown in the supplementary information.

	R_1	R_2
α	CH_3	CH_3
β	CH_3	H
γ	H	CH_3
δ	H	H

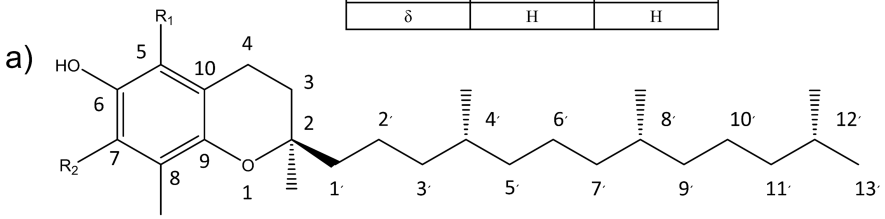

tocopherols (T)

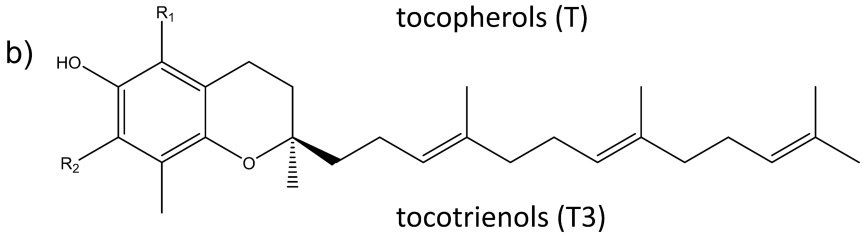

tocotrienols (T3)

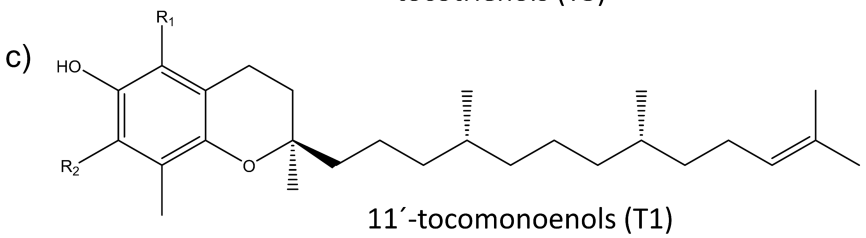

11´-tocomonoenols (T1)

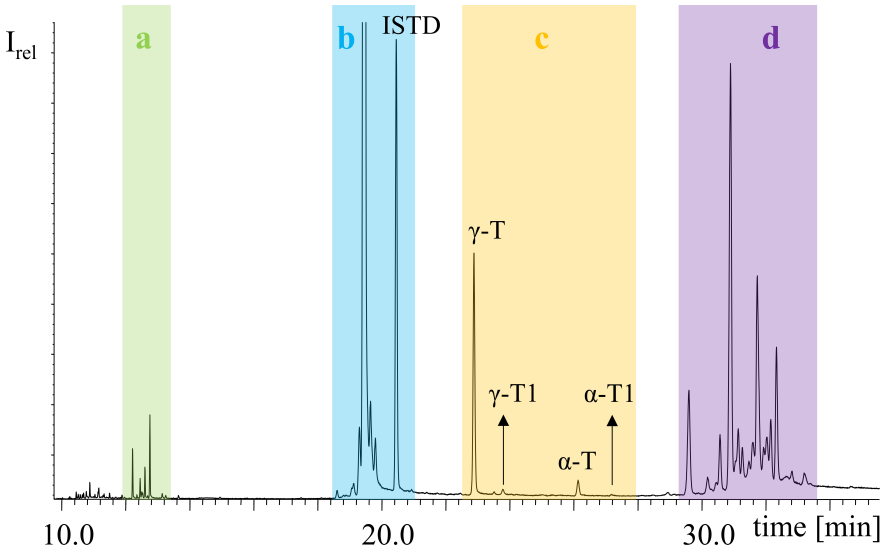

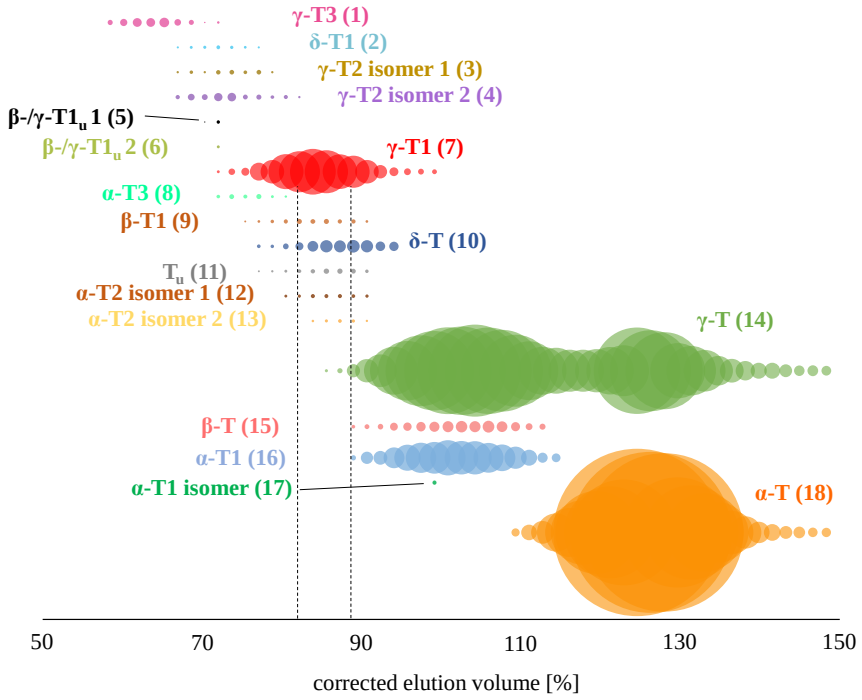

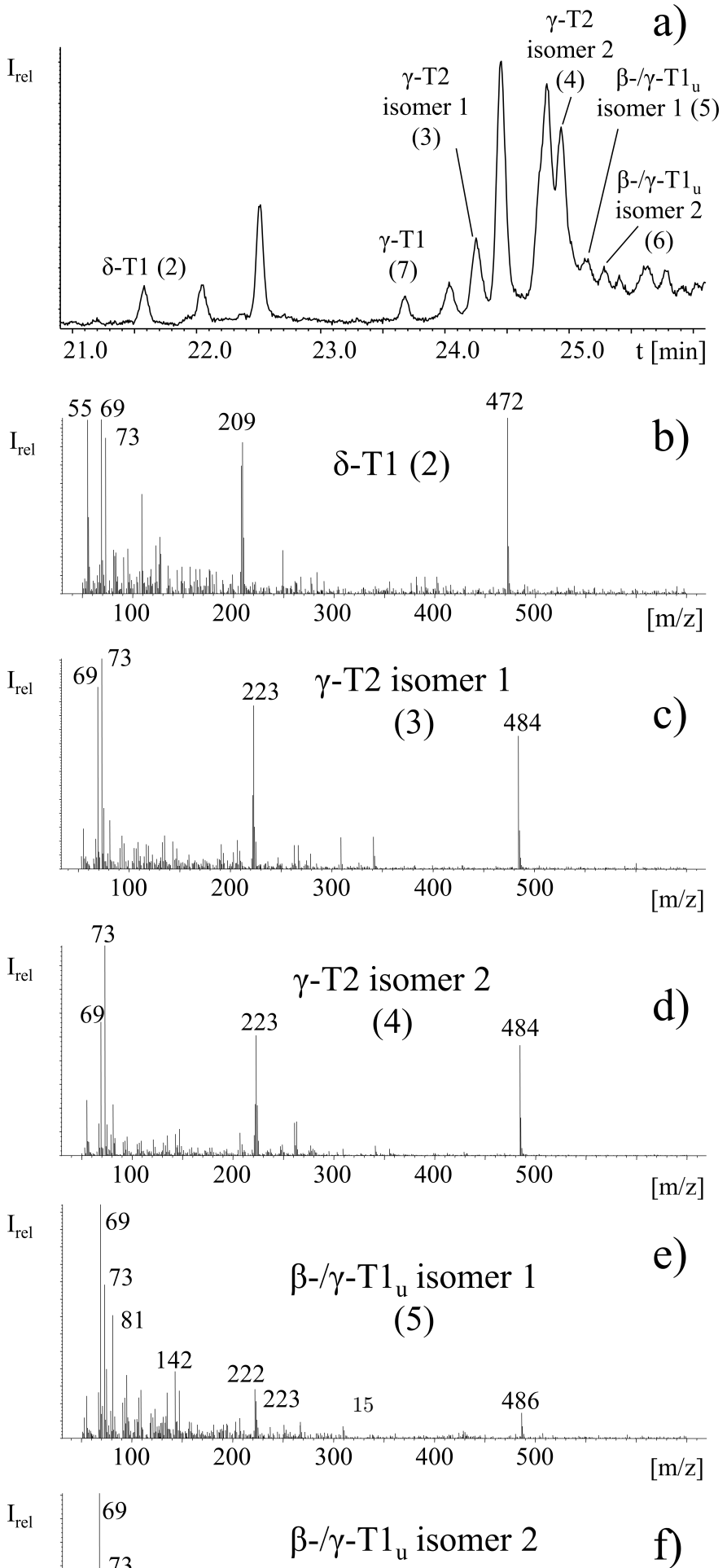

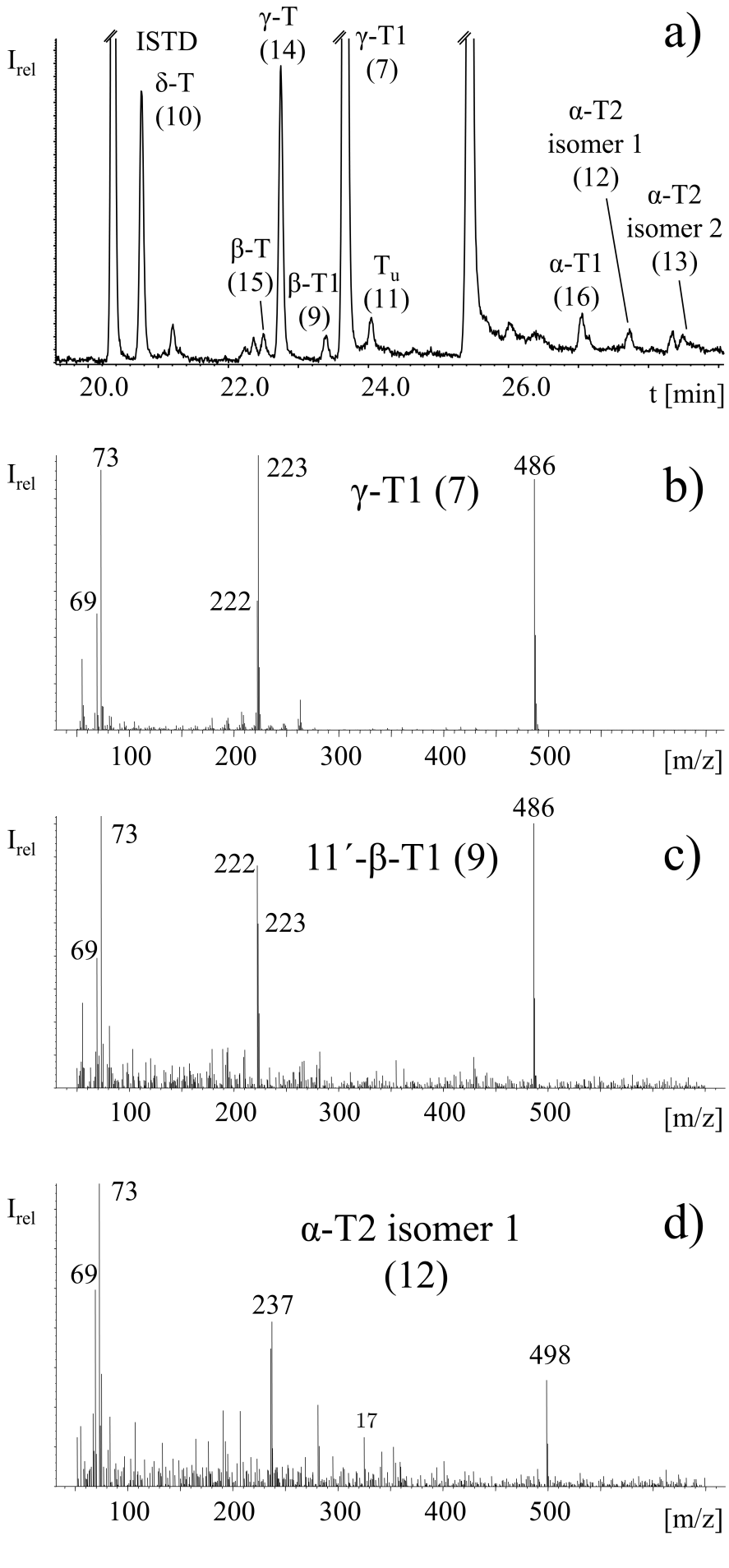

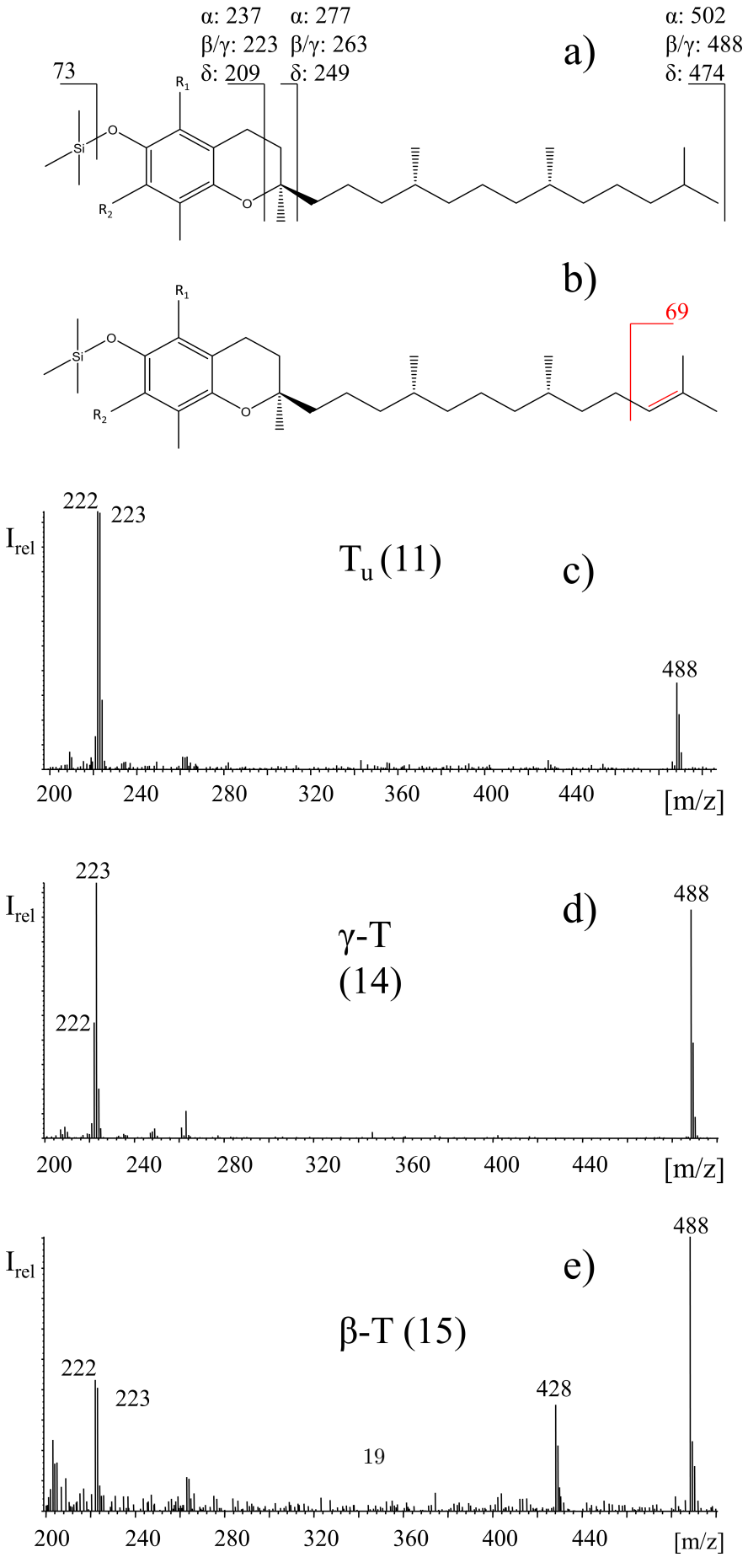

fraction	share of γ-T1
3.1	0
3.2	0.2
3.3	3.9
3.4	8.5
3.5	29.2
3.6	58.2
4	0.0

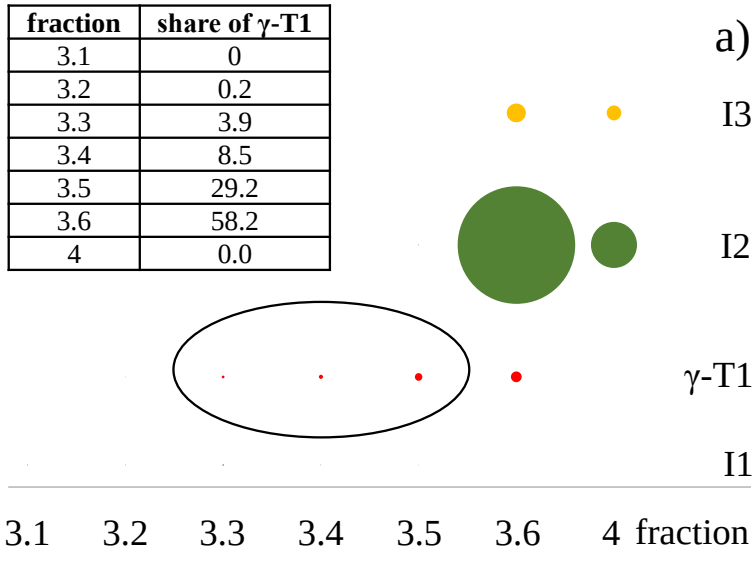

fraction	share of γ-T1
3.1	0.003
3.2	0.1
3.3	2.1
3.4	5.0
3.5	18.2
3.6	74.7
4	0.0